JARO 12: 577–594 (2011)
DOI: 10.1007/s10162-011-0269-0


JARO
Journal of the Association for Research in Otolaryngology

# Biophysical Mechanisms Underlying Outer Hair Cell Loss Associated with a Shortened Tectorial Membrane

Christopher C. Liu[1], Simon S. Gao[2], Tao Yuan[1], Charles Steele[3], Sunil Puria[3,4], and John S. Oghalai[2,4]

[1]*The Bobby R. Alford Department of Otolaryngology–Head and Neck Surgery, Baylor College of Medicine, Houston, TX 77030, USA*

[2]*Department of Bioengineering, Rice University, Houston, TX 77005, USA*

[3]*Department of Mechanical Engineering, Stanford University, Stanford, CA 94304-5739, USA*

[4]*Department of Otolaryngology–Head and Neck Surgery, Stanford University, 801 Welch Road, Stanford, CA 94305-5739, USA*

Received: 6 February 2011; Accepted: 17 April 2011; Online publication: 13 May 2011

## ABSTRACT

The tectorial membrane (TM) connects to the stereocilia bundles of outer hair cells (OHCs). Humans with an autosomal dominant C1509G mutation in alpha-tectorin, a protein constituent of the TM, are born with a partial hearing loss that worsens over time. The *Tecta*$^{C1509/+}$ transgenic mouse with the same point mutation has partial hearing loss secondary to a shortened TM that only contacts the first row of OHCs. As well, *Tecta*$^{C1509G/+}$ mice have increased expression of the OHC electromotility protein, prestin. We sought to determine whether these changes impact OHC survival. Distortion product otoacoustic emission thresholds in a quiet environment did not change to 6 months of age. However, noise exposure produced acute threshold shifts that fully recovered in *Tecta*$^{+/+}$ mice but only partially recovered in *Tecta*$^{C1509G/+}$ mice. While *Tecta*$^{+/+}$ mice lost OHCs primarily at the base and within all three rows, *Tecta*$^{C1509G/+}$ mice lost most of their OHCs in a more apical region of the cochlea and nearly completely within the first row. In order to estimate the impact of a shorter TM on the forces faced by the stereocilia within the first OHC row, both the wild type and the heterozygous conditions were simulated in a computational model. These analyses predicted that the shear force on the stereocilia is ~50% higher in the heterozygous condition. We then measured electrically induced movements of the reticular lamina in situ and found that while they decreased to the noise floor in prestin null mice, they were increased by 4.58 dB in *Tecta*$^{C1509G/+}$ mice compared to *Tecta*$^{+/+}$ mice. The increased movements were associated with a fourfold increase in OHC death as measured by vital dye staining. Together, these findings indicate that uncoupling the TM from some OHCs leads to partial hearing loss and places the remaining coupled OHCs at higher risk. Both the mechanics of the malformed TM and the increased prestin-related movements of the organ of Corti contribute to this higher risk profile.

**Keywords:** hair cell, cochlea, transduction, electromotility, hearing, deafness, hearing loss

## INTRODUCTION

Hearing loss is a disabling condition that significantly impacts quality of life. In neonates and young children, hearing loss can be devastating because it affects cognitive, language, social, and emotional development (Cristobal and Oghalai 2008; Karchmer and Allen 1999; Kushalnagar et al. 2007; Pierson et al. 2007). Slowly progressive hearing loss is a common pathway to deafness. There are currently no medical treatments to reduce the progression of hearing loss. Research in this area

*Correspondence to*: John S. Oghalai · Department of Otolaryngology–Head and Neck Surgery · Stanford University · 801 Welch Road, Stanford, CA 94305-5739, USA. e-mail: joghalai@stanford.edu

is limited because it is difficult to characterize the underlying pathophysiology in humans. Current imaging technologies are limited by inadequate resolution; tissue biopsies of the inner ear are not ethically feasible; and postmortem histological analyses are affected by artifacts. Therefore, most functional studies today use transgenic mice with human hearing loss mutations (Leibovici et al. 2008).

In the normal cochlea, sound waves vibrate the organ of Corti, producing a shearing force between the tectorial membrane (TM) and the hair cell stereocilia. The resultant bundle deflections activate mechanoelectrical transduction channels that modulate cation entry into the hair cells (for reviews see, Fettiplace 2009; Hudspeth 2008; Petit and Richardson 2009). The transmembrane potential changes stimulate outer hair cell (OHC) electromotility (somatic length changes), mediated by the membrane protein prestin (Brownell et al. 1985; Zheng et al. 2000). The role of OHC electromotility in hearing is to generate forces that increase vibrations of the organ of Corti, a phenomenon called cochlear amplification (Dallos 2008; Davis 1983; Liberman et al. 2002; Oghalai 2004a). Disruption of the cochlear amplifier due to OHC loss or dysfunction is a common cause of hearing loss (Dallos et al. 2006; Kiang et al. 1986).

Herein, we report how a transgenic mouse that has an altered TM impacts OHC survival. The *Tecta* gene, expressed transiently during cochlear development (Rau et al. 1999), encodes α-tectorin, an extracellular protein component of the TM (Goodyear and Richardson 2002). Humans with a cysteine-to-glycine substitution at codon 1509 of this gene are born with an autosomal dominant, partial hearing loss that steadily worsens with time (Pfister et al. 2004). Previously, we created a mouse model of this condition by introducing this point mutation into the *Tecta* gene (Xia et al. 2010). Characterization of this mouse model revealed that $Tecta^{C1509G/+}$ mice have a malformed TM that is shortened in the radial direction so that instead of stimulating all three rows of OHCs, it only stimulates the first row of OHCs, which results in partial congenital hearing loss. We also found that $Tecta^{C1509G/+}$ OHCs express more prestin than $Tecta^{+/+}$ OHCs.

In this report, we studied OHC loss that occurs in mature $Tecta^{C1509G/+}$ mice, and we identified two specific mechanisms that appear to play a role in adult-onset hearing loss. The first is that the TM malformation alters the shear force on the stereocilia, which changes the pattern of OHC death after noise exposure. The second is that increased prestin-related movement of the organ of Corti increases the risk of OHC death.

## METHODS

### Animals

The study protocol was approved by the Baylor College of Medicine Institutional Animal Care and Use Committee. The $Tecta^{C1509G}$ mutant mouse was created previously in our laboratory (Xia et al. 2010). Briefly, a standard homologous replacement knock-in strategy was used to create a target vector that was electroporated into AB1.2 (129/Sv/Ev) embryonic stem cells (Qiu et al. 1997). This mutation leads to a cysteine to glycine change at codon 1509 in the mouse *Tecta* gene. Age-related hearing loss genes associated with the 129/Sv/Ev background (Liberman et al. 2002; Yoshida et al. 2000) were reduced by crossing heterozygous F2 mice with wild-type CBA mice for three generations so as to reduce the 129/Sv/Ev background to 12.5%. All mice studied were littermates of the F6–F7 generations in this background and were between 3 and 5 weeks old unless otherwise stated.

### DPOAE Measurements

Mice of either sex were anesthetized with a solution of ketamine (100 mg/kg) and xylazine (5 mg/kg). Supplemental doses of anesthesia were administered to maintain areflexia with paw pinch. Distortion product otoacoustic emission (DPOAE) thresholds were measured as previously described (Xia et al. 2007). Briefly, sine wave stimuli were digitally generated with MATLAB (Version 7.9.0.529, The Mathworks, Natick, MA, USA), converted to analog signals with a 200 kHz digital-to-analog converter, and then attenuated to the appropriate intensity (RP2 and PA5, Tucker-Davis Technologies, Alachua, FL, USA; Oghalai 2004b). Acoustic stimuli for DPOAE measurements were produced by high-frequency piezoelectric speakers (EC1, Tucker–Davis Technologies) connected to an ear bar inserted into the external auditory canal. A probe-tip microphone (type 8192, NEXUS conditioning amplifier, Bruel and Kjaer, Denmark) inserted through the same ear bar was placed within 3 mm of the tympanic membrane and used to calibrate the speakers. The maximum sound pressure level (SPL) that these speakers produced ranged from 70 to 90 dB SPL over the frequency spectrum. Thresholds were calculated from the DPOAE responses for each frequency. Any frequency in which no response was measured to equipment limits was assigned a threshold value of 80 dB SPL.

### Noise Exposure Protocol

To induce hearing loss from noise exposure, awake adult mice were exposed to noise for 4 h. A cage

containing the mice was placed inside a closed box with six piezo horns (TW-125, Pyramid Car Audio, Brooklyn, NY, USA) inserted through the cover. The noise signal was created digitally with RpvdsEx software (Version 6.6, Tucker-Davis Technologies, Alachua, FL, USA), converted to analog by a digital-to-analog converter, and then transferred to the power amplifier (Servo 550, Sampson, Hauppauge, NY, USA) driving the speakers. The noise intensity inside the box was measured with a free-field microphone (type 4939, NEXUS conditioning amplifier, Bruel and Kjaer, Denmark), and it varied no more than ±2 dB SPL throughout the interior of the cage. The flat-weighted total intensity of the noise stimulus was increased to 98± 3 dB SPL by adjusting the volume knob on the power amplifier. While the digitally created signal had a flat frequency response over the range of 4–22 kHz (with >120 dB attenuation outside of this range), the measured power over the frequency spectrum varied as a result of the acoustical properties of the speakers, the box, and the power amplifier (Fig. 1).

## Phalloidin Staining of Fixed Cochlear Preparations

To assess OHC loss after noise exposure, mice were anesthetized and sacrificed by cervical dislocation 1 week after noise exposure. Their cochleae were removed and immersed in a 313±2 mOsm/kg artificial perilymph solution containing 150 mM NaCl, 5 mM KCl, 1.5 mM $CaCl_2$, 10 mM HEPES, and 10 mM glucose at pH 7.35. Under a dissecting microscope (SteREO Discover.V8, Zeiss, Germany), the vestibular structures and ossicles were carefully removed. The cochleae were then fixed in 4% paraformaldehyde at room temperature for 2 h and then glued upright into custom-built chambers. Once the cochleae were secured, the otic capsule over the basal turn was removed with a fine knife. The OHC epithelium was exposed after Reissner's membrane and the TM were removed with a pick. The cochleae were then rinsed with phosphate-buffered saline containing 0.1% Triton-X100 three times (10 min per rinse) to facilitate dye uptake. F-Actin was labeled by immersing the cochleae in Alexa Fluor 546 Phalloidin (A22283, Invitrogen; 1:200 in phosphate-buffered solution) at room temperature for 1 h.

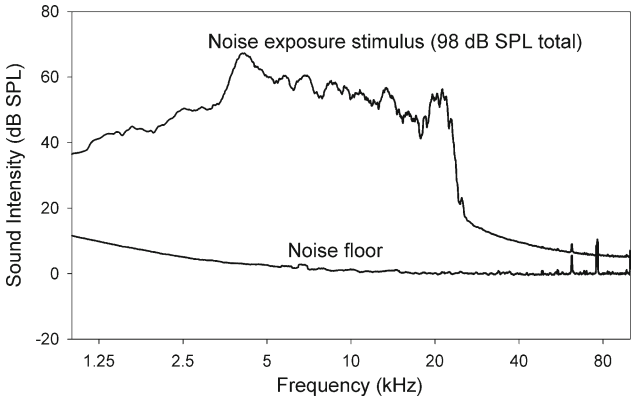


**FIG. 1.** Frequency response of the noise exposure stimulus. This was measured by placing a microphone inside the noise-exposure box. An FFT was performed after digitizing the signal and converting the units from volts to dB SPL. The noise floor was collected with the noise stimulus turned off.

Labeled cochleae were imaged using a custom-built two-photon microscope (Yuan et al. 2010). Briefly, the microscope consisted of a moveable objective microscope (Sutter) fitted with a 20× water-immersion objective (NA 0.95, XLUMPlanFl, Olympus America, Center Valley, PA, USA). A femtosecond Ti:sapphire laser (Chameleon, Coherent, Santa Clara, CA, USA) tuned to 800 nm provided two-photon excitation. The emitted fluorescence was detected by a photomultiplier tube after optical filtering (ET630/75m filter set, Chroma, Bellows Falls, VT, USA). Lateral scanning was achieved by two galvanometer-actuated mirrors controlling the laser beam. Axial scanning was achieved by a separate actuator that controlled the objective lens. A modified version of ScanImage open source software (Pologruto et al. 2003) was used to control the hardware. For each cochlea, we scanned eight regions starting from the base. Each region contained approximately 22 OHCs. The total length of cochlea scanned was approximately 1.4 mm. Phalloidin-negative gaps in the OHC rows were presumed to represent degenerated or missing OHCs (Lim et al. 2008), and the proportion of missing OHCs was calculated for each scanned region. Cytocochleograms were created with the collected data after the percent distance from the base for each region was calculated using 5.72 mm as the average length of a CBA/CaJ mouse cochlea fixed in 4% paraformaldehyde (Viberg and Canlon 2004).

## Freshly Excised Cochlear Preparations

A freshly excised cochlear preparation was used to measure reticular lamina motion and membrane compromise using propidium iodide labeling. Full details of this preparation have been previously reported (Xia et al. 2007, 2010; Yuan et al. 2010). The cochleae were harvested as described above and then glued upright (with the apex facing up) into a custom-built chamber (IsoDent, Ellman International, Oceanside, NY, USa). A section of the otic capsule bone overlying the scala vestibuli was removed with a fine knife. Reissner's membrane and the TM were gently brushed aside with a pick to expose the hair cell epithelium. The chamber was then secured in an

experimental upright microscope (Axioskop 2 FS plus, Zeiss) and the OHCs were visualized using a 40× water immersion objective (Achroplan, NA=0.8, Zeiss). The entire preparation was bathed in artificial perilymph throughout all experimental procedures.

## Measuring Electrically Evoked Movement of the Reticular Lamina

We applied an external electrical field to the excised cochlea to stimulate the OHCs. Because the electric field stimulates electromotility from all OHCs, regardless of whether the TM is attached or not, OHC row-specific effects were not assessed. A sine wave swept from 1 to 40 kHz was generated using MATLAB, converted to analog by a digital-to-analog converter, and delivered at a constant current using a linear stimulus isolator (A395, World Precision Instruments). The stimulus was delivered between two tungsten electrodes (0.005 in diameter, A-M Systems) placed on opposite sides of the cochlea within the bathing media. The actual current delivered to the cochlea was determined by measuring the voltage drop across a 1 kΩ resistor placed in-series with the circuit. The amplitude of the current decreased at higher frequencies due to the inherent low-pass filtering characteristics of the linear stimulus isolator.

Electrically evoked movements of the reticular lamina were measured with a laser Doppler vibrometer (OFV-534, Polytec propidium iodide (PI)) mounted to the trinocular port of the upright microscope. Five to ten silver-coated glass beads 15–25 μm in diameter were carefully placed on top of the reticular lamina (Conduct-O-Fil S3000-S3N, Potters Industries, Carlstadt, NJ, USA). The laser was then focused on beads located on the apical surface of OHCs to measure their vertical displacements using the digital displacement decoder (OVD-60, Polytec PI). The displacement signal and the voltage across the 1 kΩ resistor were both digitized simultaneously at 100 kHz and collected by custom software written in MATLAB. The responses from 1 to 40 kHz were then calculated by fast Fourier transform (FFT) analysis.

While OHCs are normally angled off the vertical axis and the orientation of the preparation may vary slightly between experiments, the effect of these variations on the measured vertical displacements is small because of the cosine function of the angle. Assuming all experiments had OHC angles that varied by <45°, the variations in the vertical displacements would at most be 3 dB ($20\times\log_{10}(1/\cos(45°))$).

## Propidium Iodide Labeling

To assess for OHC membrane compromise after electrical stimulation, the cochlear preparations were immersed in a 2 μg/ml working solution of PI in artificial perilymph (Molecular Probes, Oregon, USA) and incubated at room temperature for 5 min. After rinsing for 5 min, PI-labeled OHCs were visualized and counted using an upright fluorescence microscope equipped with a long pass filter set (CY3, Zeiss, Germany). For each cochlea, the proportion of PI-labeled OHCs was determined from a minimum of 75 OHCs.

## Statistical Analyses and Image Processing

Data were analyzed with Excel (Office 2007, Microsoft, Seattle, WA, USA). Plots were generated with Sigmaplot (11.0, Systat Software, San Jose, CA, USA). Statistical significance was calculated using the one-way ANOVA or the Student's two-tailed paired or non-paired $t$ test as appropriate. $P$ values less than 0.05 were considered statistically significant. All values are presented as mean±SEM. Images were formatted using ImageJ (Version 1.43, rsbweb.nih.gov/ij), Photoshop (Version 7.01, Adobe Systems Inc, San Jose, CA, USA), and GIMP (Version 2.6.8, www.gimp.org).

## Computational Model

A mathematical model simulating the TM malformation of the $Tecta^{C1509G/+}$ mouse, where the TM only contacts the first row of OHCs, was generated based on computational models of the gerbil cochlea from our previous work (Steele et al. 2009; Yoon et al. 2006, 2007, 2009). This new model was designed to calculate hair cell forces due to deviations from normal anatomy in the organ of Corti, as was done for the guinea pig (Steele et al. 2010). We used the gerbil rather than the mouse because suitable data regarding gerbil organ of Corti mechanics was readily available in the published literature.

The approach involves using a computer simulation in which most cross-sectional details of the organ of Corti can be included. However, the longitudinal motion of tissue and fluid is neglected, so the results are valid only for the long wavelength response, i.e., for frequencies less than the "best frequency", or the frequency at which the maximum response is produced for a particular section. The response of this model agrees with measurements of the normal organ of Corti under mechanical and electrical loading, and offers an explanation for the various phases and the peak splitting seen in neural responses (Steele and Puria 2005). The pressure of the basilar membrane was normalized to dimensionless units by dividing it by the input pressure of the stapes. The shear force on the stereociliary bundles was calculated as the force per unit distance in the longitudinal direction (units: $N/m$). This was normalized by dividing it by the basilar membrane

pressure multiplied by three quarters of the width of the pectinate zone (units: $N{-}m/m^2$). Full details are described elsewhere (Steele et al. 2009; Yoon et al. 2006, 2007, 2009.

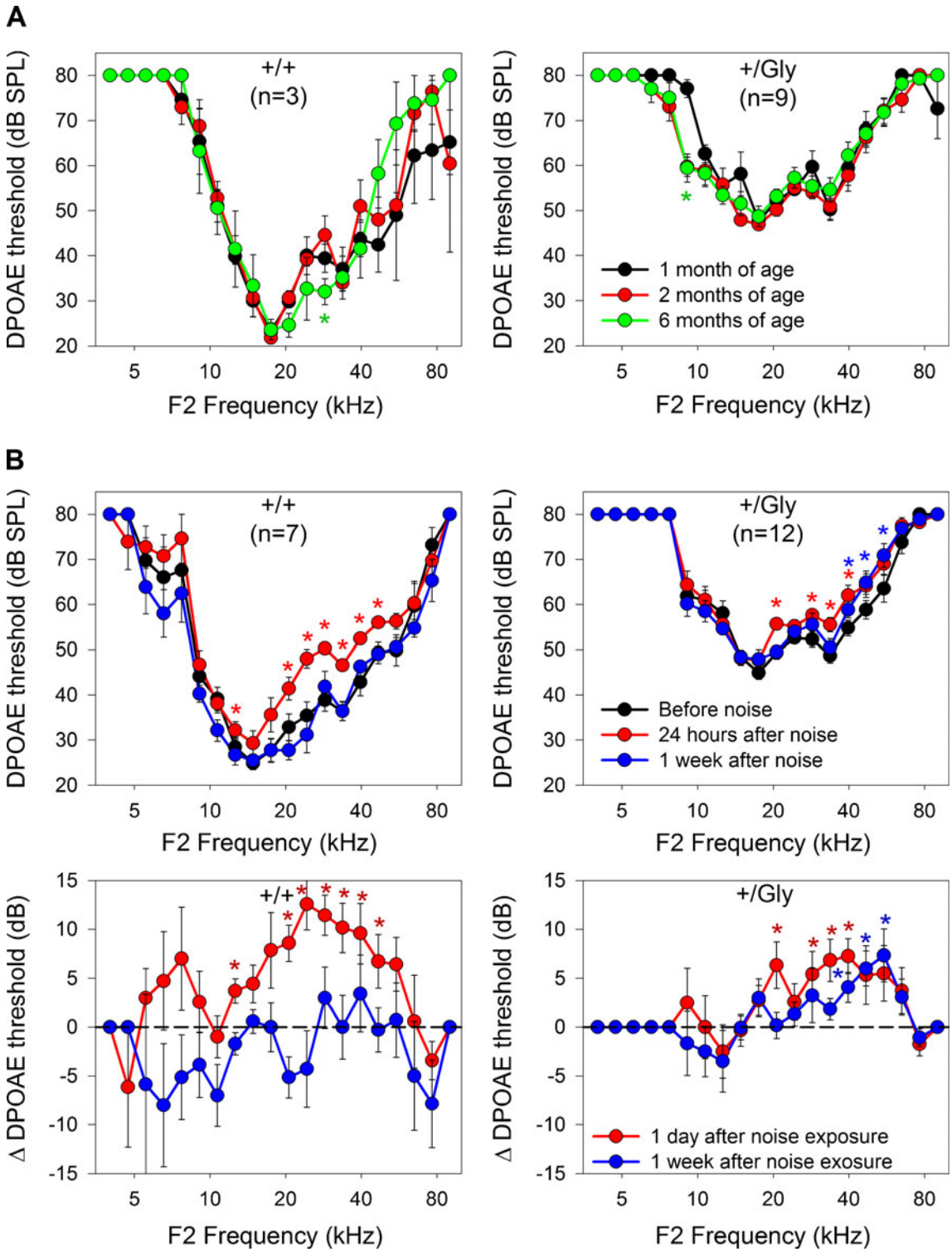


**FIG. 2.** DPOAE thresholds. **A** Cohorts of *Tecta*$^{+/+}$ (+/+) and *Tecta*$^{C1509G/+}$ (+/Gly) mice were followed for 6 months. DPOAE thresholds showed no evidence of age-related threshold increases in either wild-type or heterozygous mice during this time period. **B** Cohorts of mice were exposed to 4 h of broadband noise. One day after noise exposure, both *Tecta*$^{+/+}$ and *Tecta*$^{C1509G/+}$ mice demonstrated statistically significant threshold increases between 20 and 60 kHz (*asterisks*, paired *t* test, $p<0.05$). By 1 week, these threshold increases fully recovered in *Tecta*$^{+/+}$ mice, but only partially recovered in *Tecta*$^{C1509G/+}$ mice.

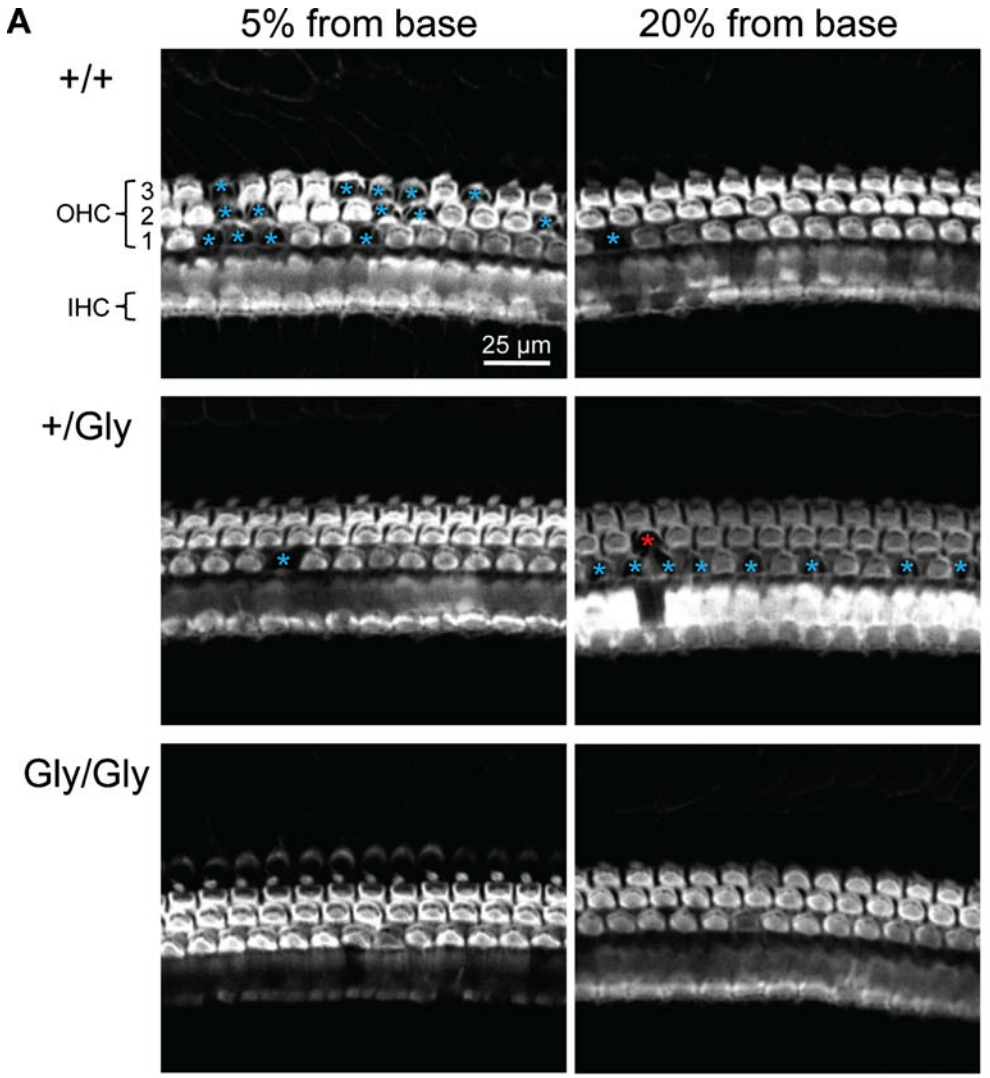
A
5% from base
20% from base
+/+
OHC
3
2
1
IHC
25 μm
+/Gly
Gly/Gly

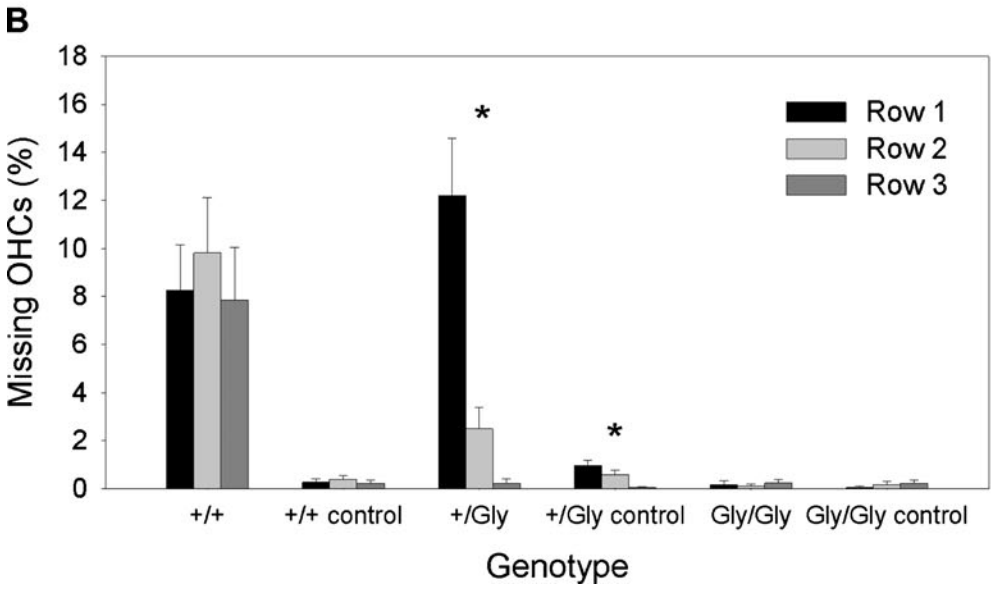
B
Missing OHCs (%)
18
16
14
12
10
8
6
4
2
0
*
*
Row 1
Row 2
Row 3
+/+
+/+ control
+/Gly
+/Gly control
Gly/Gly
Gly/Gly control
Genotype

**FIG. 3.** Outer hair cell loss after noise exposure. **A** Two-photon micrographs of phalloidin-labeled hair cell epithelia in *Tecta*$^{+/+}$ (+/+), *Tecta*$^{C1509G/+}$ (+/Gly), and *Tecta*$^{C1509G/C1509G}$ (Gly/Gly) mice 1 week after noise exposure. Images were taken at two different longitudinal locations along the cochlear partition. *Blue asterisks* demonstrate positions where OHCs are missing. The *red asterisk* points to an example of a missing OHC in the second row of a +/Gly cochlea. When this situation occurred, the adjacent first-row OHCs were always missing as well. **B** Histogram of OHC loss 1 week after noise exposure, separated by OHC row. The total proportion of missing OHCs within the first 25% of the mouse cochlea (from the base) is plotted. Noise-exposed *Tecta*$^{C1509G/+}$ mice demonstrated a preferential loss of first row OHCs (*asterisks*, $n$=10–16, ANOVA followed by $t$ test, $p<0.05$). Control mice were not exposed to noise and demonstrated little OHC loss in any genotype. *Error bars* represent the SEM.

## RESULTS

### Age-Related and Noise-Induced Changes in Cochlear Function

Because humans with the *TECTA*$^{C1509G/+}$ mutation present clinically with hearing loss that progressively worsens, we wanted to determine if *Tecta*$^{C1509G/+}$ mice demonstrate a similar pattern of hearing loss (Pfister et al. 2004). Auditory brainstem responses (ABR) were not used to assess changes in hearing acuity because the thresholds in heterozygous mice (Xia et al. 2010) are already close to the maximum stimulus intensity our sound equipment can deliver, so additional hearing loss could not be accurately detected. However, DPOAE thresholds of heterozygous mice are low enough to be effectively measured with our equipment. One additional benefit of studying DPOAEs is that they more selectively assess TM–OHC interactions, the focus of this study (Brownell 1990; Frolenkov et al. 1998). In contrast, ABR testing also assesses inner hair cell and auditory nerve stimulation. *Tecta*$^{C1509G/C1509G}$ mice, which have a TM that does not contact any of the OHC rows, have no DPOAEs to our equipment limits and were not studied.

We tested for progressive age-related decline in cochlear function by measuring DPOAE thresholds in cohorts of *Tecta*$^{+/+}$ and *Tecta*$^{C1509G/+}$ mice at 1, 2, and 6 months of age (Fig. 2A). At 1 month of age, the DPOAE thresholds in *Tecta*$^{+/+}$ and *Tecta*$^{C1509G/+}$ mice were no different than those in cohorts measured previously (Xia et al. 2010). DPOAE thresholds at 2 months of age were similar to thresholds measured at 1 month (paired $t$ test at each frequency, $p>0.05$). By 6 months of age, only one frequency in *Tecta*$^{+/+}$ (28.6 kHz) and one frequency in *Tecta*$^{C1509G/+}$ (9.1 kHz) mice demonstrated statistically significant changes. Since both of these were improvements in DPOAE thresholds and no other changes were noted over the frequency spectrum, these findings were likely a result of chance. Therefore, at least up to 6 months, age-related changes did not occur in either cohort of mice.

However, these age-related measurements were performed on mice kept in a quiet animal facility and a major contributing factor to progressive hearing loss in humans is noise exposure (Gates et al. 2000; Holme and Steel 2004; Kujawa and Liberman 2006; Ohlemiller 2008; Rosenhall 2003; Seidman et al. 2002). Therefore, we assessed for noise-induced cochlear changes in cohorts of *Tecta*$^{+/+}$ and *Tecta*$^{C1509G/+}$ mice. These mice were exposed to noise (4–22 kHz at 98±3 dB SPL) for 4 h. One day after noise exposure, statistically significant DPOAE threshold elevations in both genotypes were apparent at middle and high frequencies (Fig. 2B). One week after exposure, the cohort of *Tecta*$^{+/+}$ mice demonstrated complete recovery at all frequencies. In contrast, the cohort of *Tecta*$^{C1509G/+}$ mice demonstrated only a partial recovery and the residual threshold shift was significantly different from baseline in the F2 frequency range of 35–60 kHz. These data demonstrate that *Tecta*$^{C1509G/+}$ mice do not recover from DPOAE threshold shifts after noise exposure as well as wild-type mice.

### Noise-Induced Hearing Loss in Tecta$^{C1509G/+}$ Mice Involves OHC Loss

A frequent finding associated with noise-induced hearing loss is OHC death (Chen and Fetcher 2003). We sought to determine if *Tecta*$^{C1509G/+}$ mice lose a greater proportion of their OHCs than their wild-type littermates after noise exposure. This was accomplished by applying a phalloidin stain onto cochleae excised from mice 1 week after broadband noise exposure and counting OHCs within the basal-most 25% of the cochlea (Fig. 3A). Missing OHCs were easily identifiable as a lack of phalloidin labeling in the cuticular plate region. There was no statistically significant difference between the total amount of OHC loss in *Tecta*$^{+/+}$ and *Tecta*$^{C1509G/+}$ mice (8.6±2.1% and 5.0±1.1%, $n$=16 and 11, respectively; ANOVA, $p$=0.2). *Tecta*$^{+/+}$ mice demonstrated OHC loss among all three rows ($r1$, 8.3±1.9%; $r2$, 9.8±2.3%; $r3$, 7.8±2.2; ANOVA, $p$=0.8), and they tended to occur in clumps, whereby multiple adjacent OHCs from more than one row would be damaged. In contrast, there was a preferential loss of OHCs from the first row in *Tecta*$^{C1509G/+}$ mice ($r$ 1, 12.2±2.4%; $r$ 2, 2.5±0.9%, $r$ 3 0.2±0.2%; ANOVA followed by $t$ test, $p<0.05$). This is consistent with the fact that only OHCs from the first row are attached to the TM in *Tecta*$^{C1509G/+}$ mice. A few second row OHCs were also lost even though they are not believed to be attached to the TM. These losses were always accompanied by losses of adjacent first row outer hair cells (red asterisk in Fig. 3A). This pattern of OHC loss is likely due to mechanical coupling between

adjacent hair cells by supporting cells, the reticular lamina, and the basilar membrane (Kennedy et al. 2006; Meaud and Grosh 2010; Yu and Zhao 2009; Zhao and Santos-Sacchi 1999).

We also studied *Tecta*$^{C1509G/C1509G}$ mice, which have a TM that is not attached to any of the OHC rows, as controls. These mice demonstrated very little OHC death after noise exposure ($r$ 1, 0.2±0.2%; $r$ 2, 0.1±0.1%, $r$ 3, 0.2±0.1%, $n$=10, ANOVA, $p$=0.8). As well, none of the genotypes demonstrated substantial OHC loss when they were not exposed to noise (ranging from 0.1% to 1.0%; see controls, Fig. 3B). These data indicate that OHCs connected to the TM are subject to noise damage whereas those not connected to the TM are preserved. Thus, the *Tecta* genotype is reflected in the radial pattern of OHC loss.

There also were differences in the longitudinal patterns of OHC loss between *Tecta*$^{+/+}$ and *Tecta*$^{C1509G/+}$ mice. *Tecta*$^{+/+}$ mice demonstrated greater OHC loss more basally, whereas *Tecta*$^{C1509G/+}$ mice demonstrated greater OHC loss more apically (compare images at 5% vs. 20% from the base in Fig. 3A). To analyze this more carefully, we divided the previously counted basal half-turn of each cochlea into eight 0.18 mm segments and a cytocochleogram based on the average rate of OHC loss per region was constructed. We compared the rate of OHC loss at each segment between genotypes using the ANOVA test, followed by the Student's non-paired $t$ test when indicated. *Tecta*$^{+/+}$ mice demonstrated greater rates of OHC loss compared to *Tecta*$^{C1509G/+}$ mice near the base of the cochlea (Fig. 4A). Because only the first row of OHCs in *Tecta*$^{C1509G/+}$ mice come in contact with the TM, cytocochleograms were also plotted by OHC row (Fig. 4B). In row 1, *Tecta*$^{+/+}$ mice lost fewer OHCs than *Tecta*$^{C1509G/+}$ mice when the distance from the base was between 18% and 25% (non-paired Student's $t$ test, $p$<0.05). On the other hand, *Tecta*$^{+/+}$ mice lost more OHCs in rows 2 and 3 compared to *Tecta*$^{C1509G/+}$ mice near the base of the cochlea (non-paired Student's $t$ test, $p$<0.05).

When only OHCs that are in contact with the TM are analyzed (all three rows in *Tecta*$^{+/+}$ and only the first row in *Tecta*$^{C1509G/+}$ mice), the differences in the patterns of OHC loss in *Tecta*$^{C1509G/+}$ and *Tecta*$^{+/+}$ mice were even more obvious (Fig. 5). The area of the cochlear partition most affected in *Tecta*$^{C1509G/+}$ mice corresponds to the region of the cochlea that is most sensitive to frequencies between 39 and 48 kHz (Muller et al. 2005). This frequency range falls roughly within the same frequency range of residual DPOAE threshold shifts in *Tecta*$^{C1509G/+}$ mice 1 week after noise exposure ($F$2=35–60 kHz). Taken together, these data demonstrate that OHC loss in *Tecta*$^{+/+}$ mice is highest at the base and declines at more apical locations. In contrast, *Tecta*$^{C1509G/+}$ mice lose larger numbers of TM-attached OHCs in the middle region of the cochlear partition. As expected, *Tecta*$^{C1509G/C1509G}$ mice did not lose substantial numbers of OHCs at any location. Thus, the *Tecta* genotype was also reflected in the longitudinal pattern of OHC loss.

## Mathematical Model of the Forces Applied onto the OHC Stereocilia

We simulated the normal wild-type mouse TM (Fig. 6A) and the shortened heterozygous TM using our mathematical model. We simply changed the TM so that it was only attached to the first row of OHCs, and no adjustments to any other parameters were made. Noise was simulated as a sum of BM traveling wave amplitude curves (Fig. 6B, C). The shear forces between the TM and the tall cilia, normalized by the pressure and multiplied by the BM width, were calculated for OHC rows 1, 2, and 3, respectively, for the wild type and for just the one row of the heterozygous condition (Fig. 6D, E). Note the substantially higher shear force for the heterozygous condition at the base, mid-turn, and apex of the cochlea. As well, the shear force was nearly equal at the base and middle of the cochlea. In contrast, the shear force for row 1 of the wild-type cochlea was lower at the middle and apex compared to at the base.

We then allowed for the possibility that the mutation altered the biophysical properties of the TM, as has been previously reported for another *Tecta* mutant mouse (Masaki et al. 2010). Thus, we tested the effect of reducing the elastic modulus of the TM by a factor of 10 in the heterozygous model. This change resulted in higher stress levels in the middle region of the heterozygous cochlea compared to the wild-type scenario (Fig. 6F). Thus, computational modeling supports the concept that OHCs within the first row are subject to higher stress levels when stimulated by a malformed TM than by a normal TM, and that this elevation in stress is largest in the middle region of the heterozygous cochlea.

## Increased Electrically Evoked Movements of the Reticular Lamina in Tecta$^{C1509G}$ Mutant Mice

Previous reports have demonstrated that OHCs are vulnerable to excess electromotility (Brownell 1986; Evans 1990). In particular, the OHC plasma membrane has been identified as a structure that is particularly sensitive to mechanical alteration (Chertoff and Brownell 1994; Morimoto et al. 2002; Oghalai et al. 1998, 1999, 2000; Zhi et al. 2007). Therefore, we hypothesized that one potential factor underlying the differential susceptibility of OHCs to noise between the

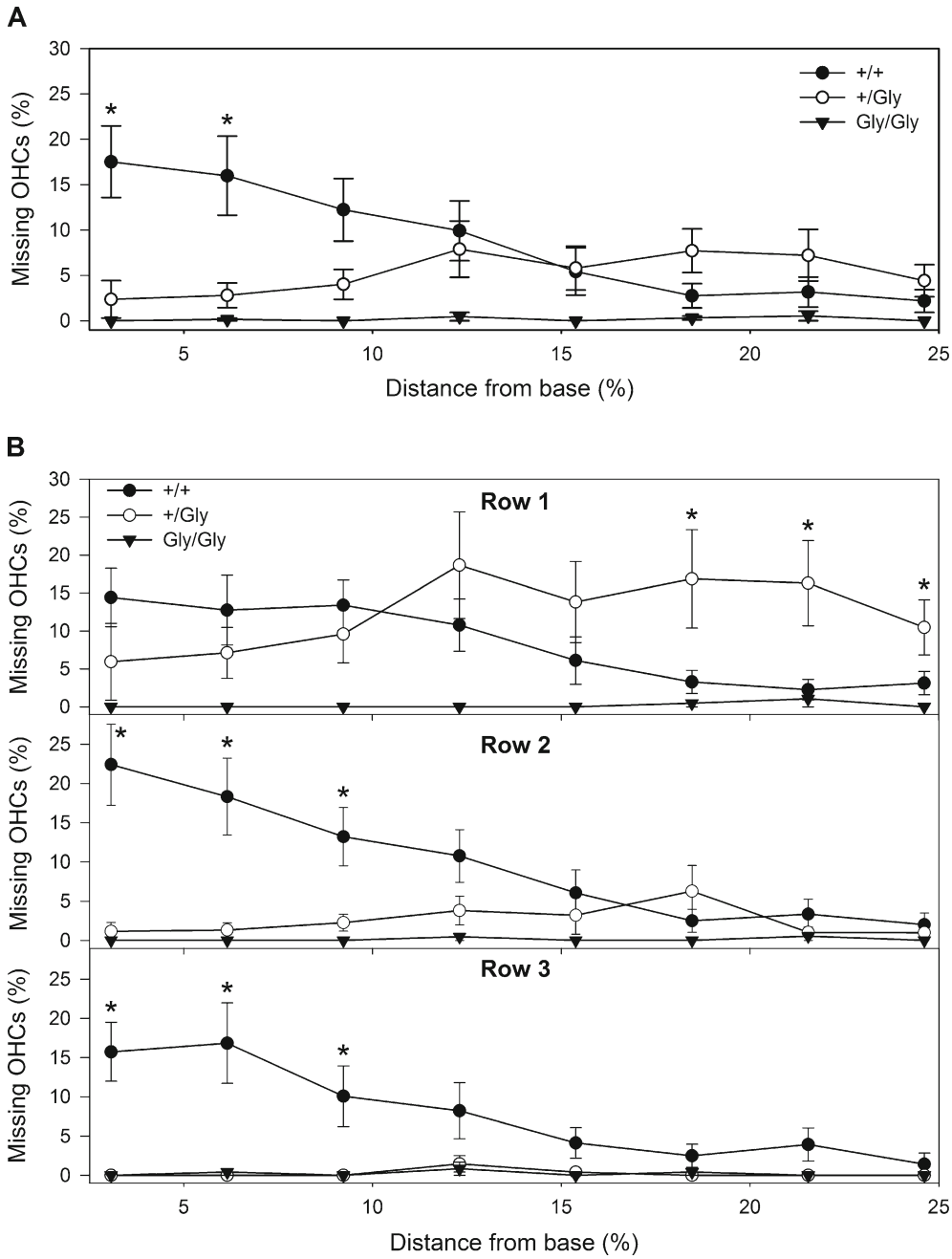


**FIG. 4.** Cytocochleograms of phalloidin-labeled cochleae 1 week after noise exposure. **A** Data from Fig. 3 was reorganized into a cytocochleogram comparing the proportion of OHCs lost in all three OHC rows between all the *Tecta* genotypes. $Tecta^{+/+}$ (+/+) mice lost a greater total proportion of OHCs compared to $Tecta^{C1509G/+}$ (+/Gly) near the base of the cochlea. Statistical significance is indicated by *asterisks* ($n$=10–16, ANOVA followed by non-paired Student's $t$ test, $p<0.05$). **B** Cytocochleograms stratified by OHC row. $Tecta^{+/+}$ (+/+) mice lost a greater proportion of Row 2 and 3 OHCs than $Tecta^{C1509G/+}$ (+/Gly) mice near the base. $Tecta^{C1509G/+}$ mice lost a greater proportion of first row OHCs in more apical regions of the basal turn of the cochlea. $Tecta^{C1509G/C1509G}$ (Gly/Gly) lost very few scattered OHCs. Statistical significance is indicated by asterisks ($n$= 10–16, non-paired Student's $t$ test, $p<0.05$).

genotypes is that $Tecta^{C1509G/+}$ and $Tecta^{C1509G/C1509G}$ OHCs have more prestin than $Tecta^{+/+}$ OHCs (Xia et al. 2010). We sought to assess OHC electromotility by measuring movements of the reticular lamina, which is mechanically coupled to the apical surfaces of the OHCs (Chan and Hudspeth 2005a; Kennedy et al. 2006; Reuter et al. 1992; Tomo et al. 2007).

We used laser Doppler vibrometry to measure the displacement of reflective beads placed on top of the reticular lamina while applying an electrical stimulus across the cochlea (Fig. 7). The alternating current stimulus varied from 1 to 40 kHz and the actual current delivered to the preparation was calculated from the measured voltage drop across a resistor in

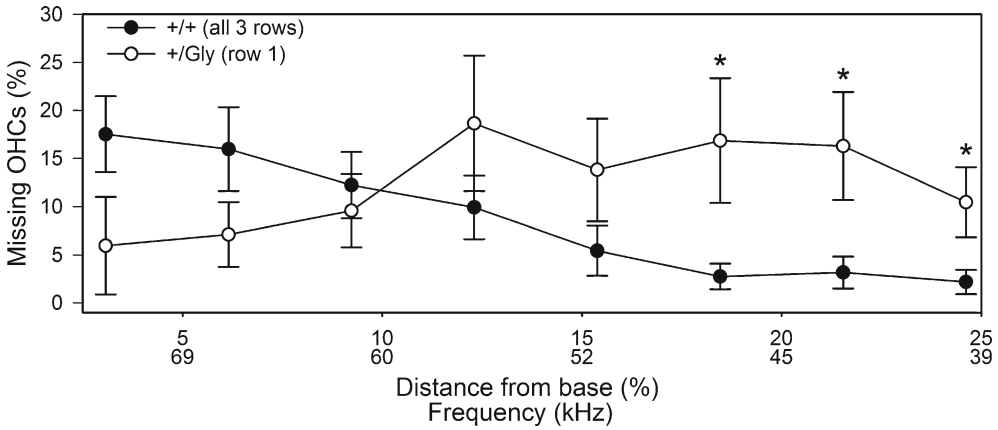


**FIG. 5.** Cytocochleogram comparing loss of OHCs in contact with the tectorial membrane in *Tecta*$^{+/+}$ and *Tecta*$^{C1509G/+}$ cochleae 1 week after noise exposure. Data from Fig. 4 was reorganized into a cytocochleogram comparing the proportion of OHCs in contact with the tectorial membrane that are lost in noise-exposed *Tecta*$^{+/+}$ (+/+) mice (all three rows of OHCs) and *Tecta*$^{C1509G/+}$ mice (only the first row of OHCs). *Tecta*$^{C1509G/+}$ mice lost a greater proportion of OHCs than *Tecta*$^{+/+}$ mice in regions 18–25% from the base of the cochlea. This region of OHC loss is sensitive to sound from 39 to 48 kHz (see *x*-axis labels), which correlates with the residual DPOAE threshold shifts in *Tecta*$^{C1509G/+}$ mice 1 week after noise exposure (*blue asterisks* in Fig. 2B). *Error bars* represent the SEM. Statistical significance is indicated by *asterisks* (*t* test, $p<0.05$).

series with the circuit. To account for variations in stimulus intensity across the studied frequency range and between cochlear preparations, we divided the bead displacement by the amplitude of the applied stimulus (expressed as dB re 0.001 nm/mA; Fig. 8).

While there was variability among different preparations (Fig. 9A), across most of the tested frequency spectrum OHCs from *Tecta*$^{C1509G/+}$ and *Tecta*$^{C1509G/C1509G}$ mice generally produced greater electrically evoked reticular lamina movements compared to those from *Tecta*$^{+/+}$ mice. The average increase, which was consistent over most of the tested frequency spectrum, was 4.58±0.25 dB and 4.83±0.15 dB for *Tecta*$^{C1509G/+}$ and *Tecta*$^{C1509G/C1509G}$ mice, respectively (Fig. 9B, ANOVA followed by *t* test, $p<0.05$ for both). Despite normalizing for the stimulus amplitude, there was a consistent decrease with frequency in every preparation. This presumably reflects a frequency dependence to the cell impedance secondary to the capacitive component of the cell membrane. Thus, the cellular transmembrane potential changes induced by the application of external AC current are predicted to drop off at higher frequencies.

Control measurements were also made. We verified that the preparation was securely fixed by measuring the displacement of beads placed on the osseous spiral lamina of *Tecta*$^{+/+}$ mice. These measurements were at the noise floor. The magnitude of movements measured from OHCs in *Prestin*$^{-/-}$ mice were also at the noise floor. Therefore, the electrically evoked movements we measured from the apical surface of OHCs were not artifacts and were prestin-dependent. Whether the increased reticular lamina motion we measured within the sensory epithelium of *Tecta*$^{C1509G}$ mutant mice is due to increased OHC electromotility resulting from their increased prestin content, or due to the mutation additionally causing a decrease in stiffness of another structure within the organ of Corti, is unknown.

## Increased Movement of the Reticular Lamina Compromises OHCs

We assessed for OHC membrane damage associated with reticular lamina motion by testing the ability of OHCs to exclude PI, a vital dye, immediately after the electrical stimulation protocol (Fig. 10A–F). The proportion of membrane-compromised OHCs that demonstrated PI labeling was calculated from fields containing a minimum of 75 OHCs per cochlea. The proportions of OHCs labeled with PI in *Tecta*$^{C1509G/+}$ (42.3±5.5%, $n$=11) and *Tecta*$^{C1509G/C1509G}$ (26.5±3.8%, $n$=11) cochleae were greater compared to *Tecta*$^{+/+}$ cochleae (10.5±2.7%, $n$=12, ANOVA followed by *t* test, $p<0.05$, Fig. 10G). Interestingly, *Prestin*$^{-/-}$ cochleae demonstrated similar rates of PI labeling (9.0±2.2%, $n$=11) to *Tecta*$^{+/+}$ cochleae. However, fewer OHCs in *Prestin*$^{-/-}$ cochleae were labeled when compared to *Tecta*$^{C1509G/+}$ and *Tecta*$^{C1509G/C1509G}$ cochleae (ANOVA followed by *t* test, $p<0.05$).

Two sets of control experiments were conducted: (1) cochleae were labeled with PI immediately after dissection without stimulus application ($n$=12–13 for each genotype) and (2) cochleae were labeled after being bathed in artificial perilymph without electrical stimulation for 16 min—the time required to complete the electrical stimulation paradigm ($n$=10–13 for each genotype). The former determined if cells were being labeled due to dissection-related trauma

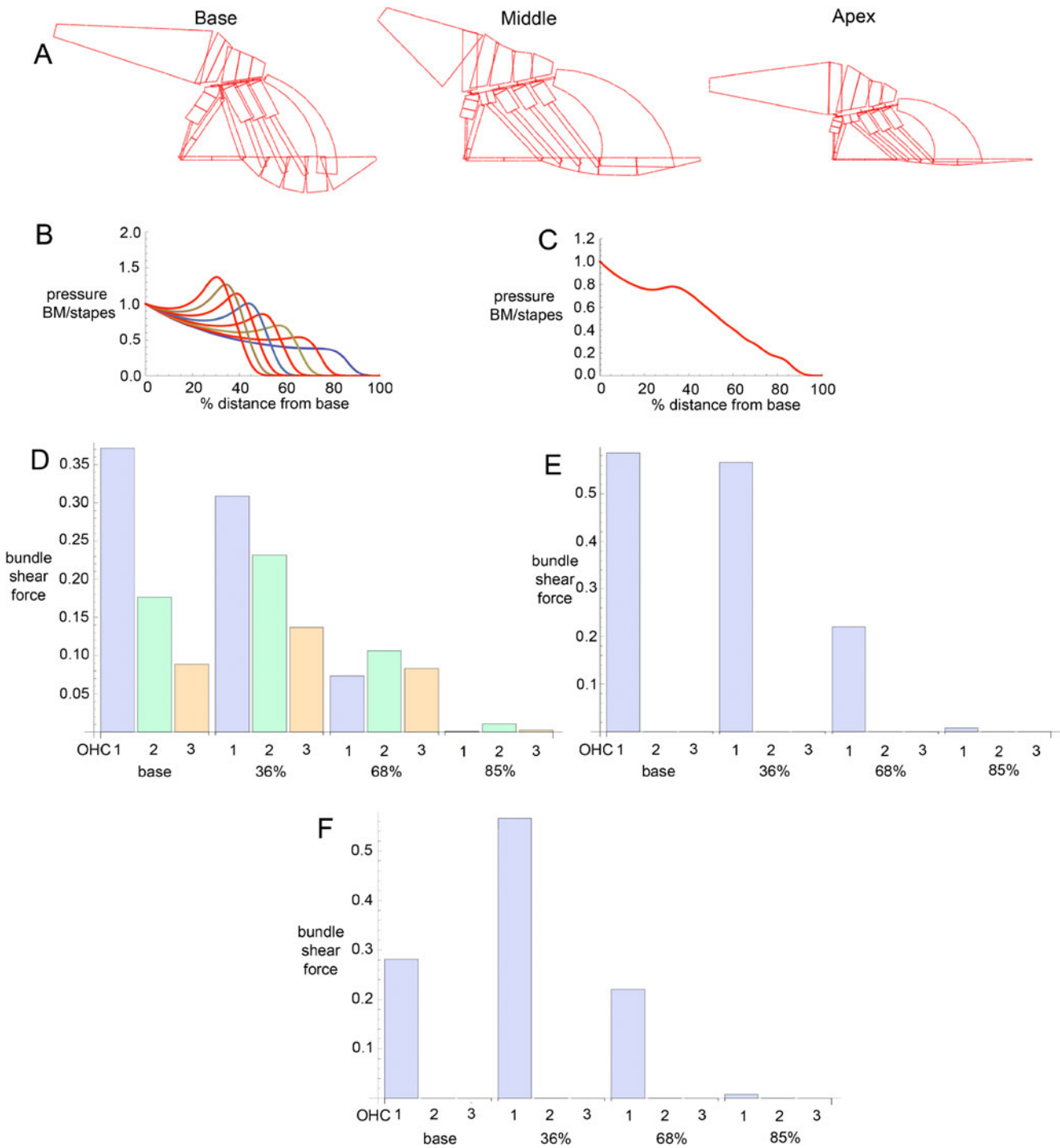


**FIG. 6.** Model calculations of the hair cell shear force for the wild-type and heterozygous conditions. **A** Cross-sections of the finite element model of the organ of Corti at three different locations. **B** Pressure at the basilar membrane normalized by the pressure input at the stapes for eight frequencies used together to simulate input noise within the 4–20 kHz frequency range. **C** The total pressure at the BM normalized by the total pressure at the stapes due to summing the eight input frequencies. **D** The normalized shear force on the hair bundles in OHC rows *1*, *2*, and *3* at the base, and at positions 36%, 68%, and 85% of the way along the length of the cochlea for the wild-type condition. **E** The normalized shear force on the hair bundles in OHC row *1* for the heterozygous condition. **F** The normalized shear force on the hair bundles in OHC row 1 for the heterozygous condition, assuming a reduction in the elastic modulus of the TM by a factor of 10.

and the latter determined if the length of time a cochlea remained immersed in artificial perilymph significantly affected OHC membrane integrity. Both sets of controls demonstrated significantly lower rates of PI labeling compared to electrically stimulated cochleae of the same genotype (all non-paired Student's $t$ tests, $p<0.05$). Together, these data suggest that the higher rates of membrane-compromised OHCs in *Tecta*$^{C1509G}$

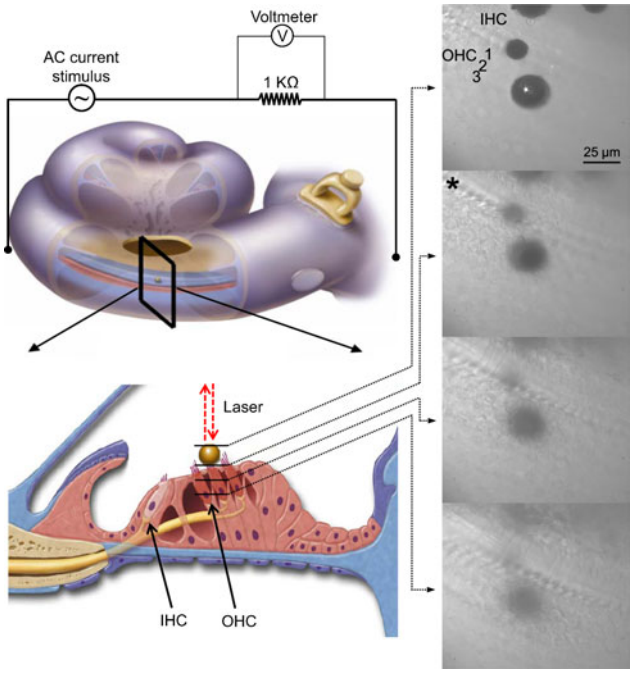


**FIG. 7.** Measuring electrically evoked movements of the reticular lamina. This is a diagrammatic representation of the experimental preparation. An opening was created in the otic capsule of an excised mouse cochlea. The TM was removed and a silver-coated glass bead was placed on top of the reticular lamina. The OHCs were uniformly stimulated by an alternating current stimulus applied across the cochlea. The applied stimulus amplitude was determined by measuring the voltage drop across an inline 1 kΩ resistor. Hyperpolarization and depolarization of the OHC initiates prestin-mediated electromotility which moves the reticular lamina. The resultant bead displacements were measured by laser Doppler vibrometry. Transmitted light images through the microscope at different planes of focus show the bead on top of the OHCs in a *Tecta*$^{+/+}$ cochlea (*right*). The TM has been removed, so it is not visible when the microscope is focused to the plane between the bead and the OHC stereocilia (*asterisk,* second image down). The illustrations are not drawn to scale.

mutant cochleae result from above-normal levels of electrically stimulated reticular lamina motion.

## DISCUSSION

Herein, we report experimental data that highlight the critical importance of the biophysical nature of the TM-OHC interactions in hearing and in hearing loss. Furthermore, we describe an organ of Corti model that mathematically simulates this malformation and supports the notion that while uncoupling of the TM from some OHCs leads to partial hearing loss, it also puts the OHCs that remain coupled at higher risk. Finally, we addressed the question of whether the increased prestin levels in the mutant are potentially relevant to the hearing loss. We found that electrical stimulation led to greater reticular lamina displacements in Tecta$^{C1509G/+}$ mice and was associated with an increased rate of OHC membrane compromise. Thus, both the mechanics of the malformed TM and increased OHC movements appear to contribute to this higher risk profile.

The pattern of OHC loss is different in the radial direction across rows, consistent with the altered TM anatomy in which only the first row of OHCs is stimulated. The pattern is also different longitudinally along the length of the cochlear partition, in that higher levels of OHC loss are not found at the extreme base but in the middle region. This is consistent with the midfrequency hearing loss (the so-called "cookie bite" audiogram) that is commonly found in patients with many different types of *TECTA* mutations (Alasti et al. 2008; Collin et al. 2008; Govaerts et al. 1998; Iwasaki et al. 2002; Kirschhofer et al. 1998; Moreno-Pelayo et al. 2001; Plantinga et al. 2006; Verhoeven et al. 1998). Therefore, we consider it likely that the mechanisms of OHC loss described in this report are pertinent to the progressive hearing loss phenotype found in humans with *TECTA* mutations.

According to our model, the reason for this altered longitudinal pattern of OHC loss in *Tecta*$^{C1509G/+}$ mice, whereby OHCs at the base are relatively spared compared to those located more apically, reflects the impact of biomechanical changes within the mutant TM. These changes are predicted to alter the pattern of OHC stereociliary stimulation along the cochlear partition (Gavara and Chadwick 2009; Gu et al. 2008; Gueta et al. 2006, 2007, 2008; Masaki et al. 2010; Meaud et al. 2010; Shoelson et al. 2004). As well, this may represent a shift in the tonotopic map of the cochlea secondary to altered TM and OHC stiffness gradients (Choi and Oghalai 2008; Deo and Grosh 2004; Ghaffari et al. 2007; He et al. 2003; Liu and Neely 2009; Masaki et al. 2009; Richter et al. 2007; Sfondouris et al. 2008; Stasiunas et al. 2009) or reduced gain of the cochlear amplifier (Oghalai 2004a).

Clinically, humans with the *TECTA*$^{C1509G/+}$ mutation are born with a partial hearing loss that progressively worsens. It is unclear whether the progressive hearing loss in humans with this mutation is due to age alone or to noise exposure. While *Tecta*$^{C1509G/+}$ mice did not experience age-related DPOAE threshold shifts out to 6 months, these mice were maintained in a quiet animal facility environment and 6 months may not be enough time for them to manifest signs of progressive sensorineural hearing loss. Nevertheless, noise exposure contributes to progressive hearing loss in humans (Gates et al. 2000; Holme and Steel 2004; Kujawa and Liberman 2006; Ohlemiller 2008; Rosenhall 2003; Seidman et al. 2002), and we found that *Tecta*$^{C1509G/+}$ mice were more susceptible to noise-induced DPOAE threshold shifts and loss of TM-coupled OHCs than *Tecta*$^{+/+}$ mice. Associated with these findings was an increase in reticular lamina motion of about 4.6–5.0 dB (~70–

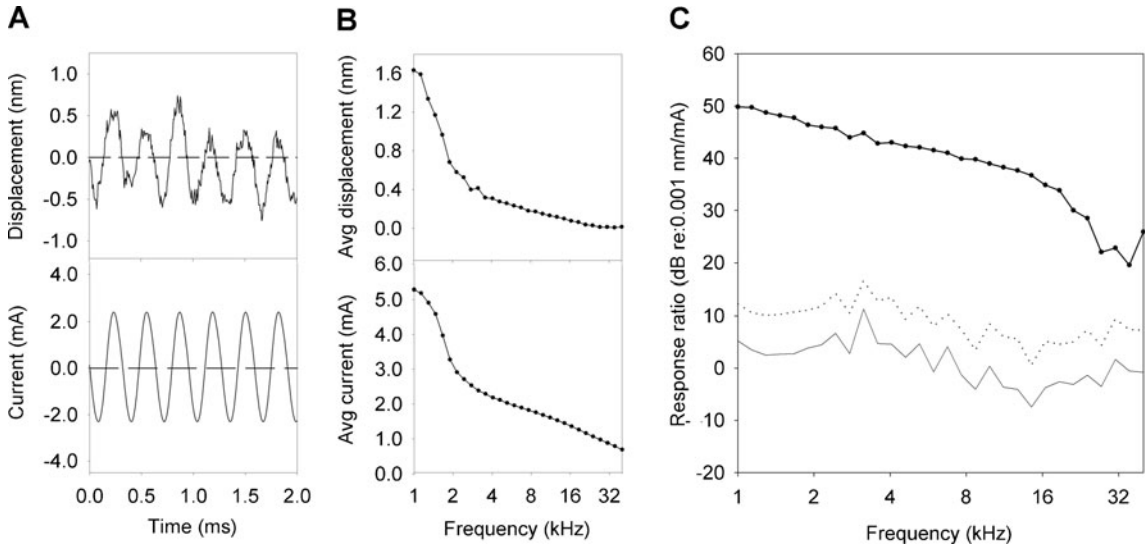


**FIG. 8.** Laser Doppler vibrometry recordings from a representative *Tecta*$^{C1509G/+}$ mouse. **A** Raw data tracings using a 3.1 kHz stimulus. *Top* bead displacement measured by the laser Doppler vibrometer before fast Fourier transform (FFT) analysis. *Bottom* the applied current calculated by measuring the voltage across the 1 kΩ resistor. The data was shifted in time to account for the time delay of the vibrometer circuitry. **B** *Top* peak bead displacement over the frequency range of 1–40 kHz. Each point represents the average of one hundred 150 ms stimuli. *Bottom* the peak applied current stimulus. The stimulus amplitude declined at higher frequencies due to equipment limitations. **C** Normalization of the displacement by the applied stimulus. The thin solid line represents the mean noise floor and the *dotted line* represents 3 SD above the noise floor.

80%) that resulted in an increased risk of membrane compromise after electrical stimulation. Taken together, these findings provide insight into the pathophysiological changes that underlie hearing loss in humans with *TECTA* mutations. Increased OHC susceptibility to chronic acoustic trauma may be the primary mechanism by which humans with the *TECTA* mutations develop progressive hearing loss.

Acoustic trauma is commonly thought to produce acute hearing loss when the process of forward transduction produces stereociliary damage (Chen et al. 2003; Chan and Hudspeth 2005b; Clark and Pickles 1996; Davis et al. 2003; Kurian et al. 2003; Lim 1986; Sakaguchi et al. 2009), increases intracellular calcium (Chan and Hudspeth 2005b; Hackney et al. 2005; Minami et al. 2004; Szonyi et al. 2001; Vicente-Torres and Schacht 2006; Yuan et al. 2010), and/or separates the tectorial membrane from the OHC stereocilia (Canlon 1987; Canlon 1988; Nordmann et al. 2000). Our previous calcium imaging data and cochlear microphonic recordings support the hypothesis that forward transduction within the first row of OHCs is similar between *Tecta*$^{+/+}$ and *Tecta*$^{C1509G/+}$ mice (Xia et al. 2010). Thus, we initially anticipated that OHCs within the first row of *Tecta*$^{C1509G/+}$ mice would be at similar risk of death to those of *Tecta*$^{+/+}$ mice after noise exposure. We also considered it possible that the risk of OHC death would be lower because the malformed TM might be able to separate from the stereocilia more easily during noise exposure. While we cannot rule out the possibility that the malformed TM can indeed separate more easily from the OHCs, experimentally we found that a greater proportion of tectorial membrane-attached OHCs were lost after noise exposure in the *Tecta*$^{C1509G/+}$ mice with the shortened TM. As well, our model predicts that OHC trauma after noise exposure is more likely to occur when the TM is malformed because not all three rows of OHCs are able to share the load of the applied force. Thus, detachment of the TM from some OHCs not only directly causes hearing loss by reducing the number of OHCs that drive the cochlear amplifier, but also puts the remaining attached OHCs at increased risk of trauma (Chen et al. 2003).

Our previous work with this mouse model demonstrated increased OHC prestin expression and greater electrically evoked otoacoustic emissions (EEOAEs) in heterozygous mice (Xia et al. 2010). These were indirect measurements of OHC electromotility. In this study, we more directly assessed electromotility by measuring movement of the reticular lamina and demonstrated enhanced electrically evoked displacements. We used the identical stimulus used previously for measuring EEOAEs (Xia et al. 2010). Importantly, there was a strong correspondence between the increased electrically evoked reticular lamina movements measured ex vivo and the increased EEOAEs measured in vivo in *Tecta*$^{C1509G/+}$ mice. Both were roughly 4–5 dB larger than *Tecta*$^{+/+}$ mice at all tested frequencies. This also compares favorably to an approximate doubling of OHC prestin expression previously found in *Tecta*$^{C1509G/+}$ mice. Our data contrasts with a previous study by Yu et al. which demonstrated an 18% increase in electromotility that was associated

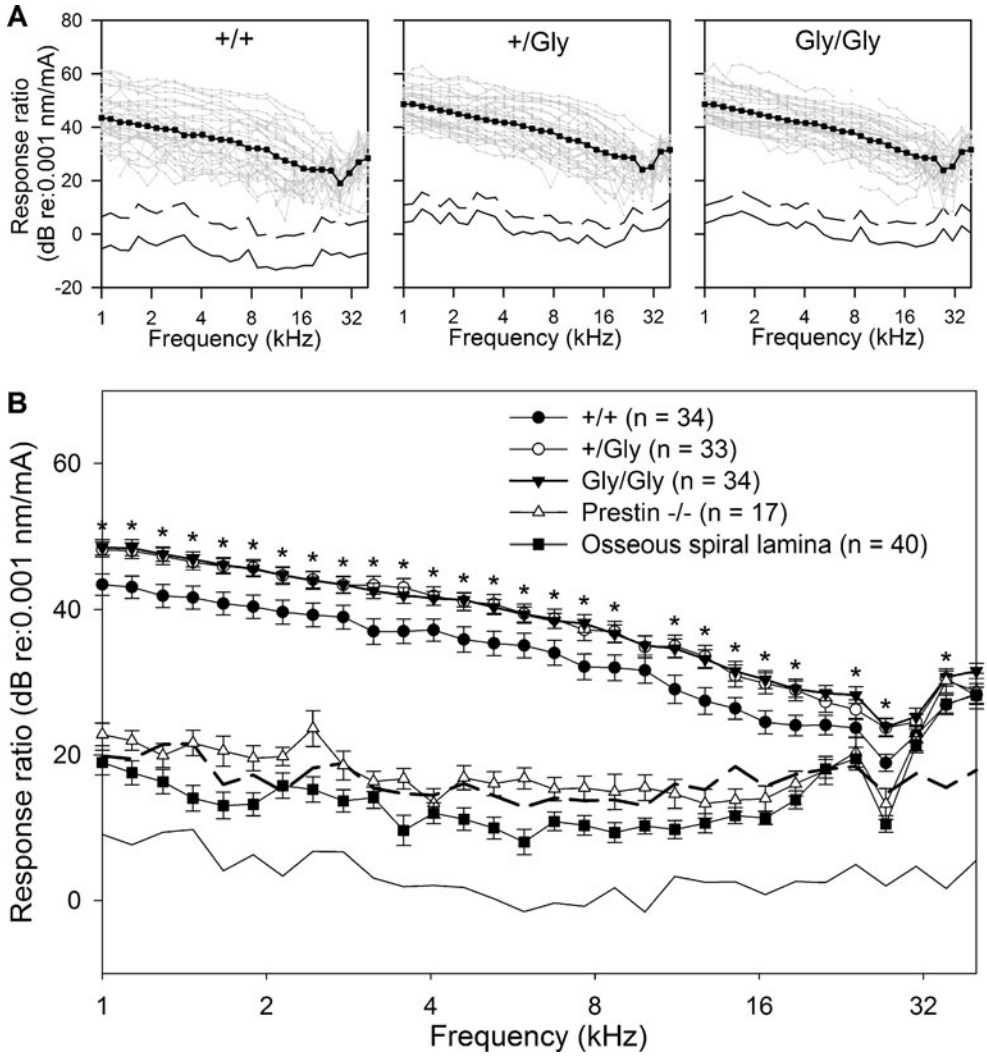


**FIG. 9.** Electrically evoked movements of the reticular lamina. Displacements of beads placed on the apical surface of OHCs within intact, freshly dissected cochleae were measured by laser Doppler vibrometry. The magnitudes of bead movements were normalized by the amplitude of the electrical stimulus. **A** Magnitude plots of the response ratios by genotype. *Gray lines* represent tracings from individual cochlear preparations. *Dark black lines* represent the average. The responses are all well above the noise floor. **B** *Tecta*$^{C1509G/+}$ (+/Gly) and *Tecta*$^{C1509G/C1509G}$ (Gly/Gly) cochleae produced greater average bead displacement compared to *Tecta*$^{+/+}$ (+/+) cochleae across most of the frequency spectrum (*asterisks,* ANOVA followed by non-paired Student's *t* test, $p<0.05$). The *solid black line* represents the mean noise floor and the dotted line represents 3 SD above the noise floor. Beads placed on top of the osseous spiral lamina in *Tecta*$^{+/+}$ mice and OHCs from *Prestin* null (*Prestin*$^{-/-}$) mice demonstrated no consistent displacements above the noise floor. *Error bars* represent the SEM.

with a fourfold increase in salicylate-induced prestin expression (Yu et al. 2008). However, salicylate is ototoxic and has been shown to eliminate OHC electromotility and alter OHC lateral wall stiffness (Lue and Brownell 1999; Peleg et al. 2007). While the increases in electromotility in *Tecta*$^{C1509G}$ mutant mice are likely due to increased functional prestin protein, we cannot rule out the possibility that alterations in supporting cell mechanics affect the expression of electromotility within the confines of the hair cell epithelium. Patch clamp studies of isolated OHCs could be performed to assess for this possibility but are beyond the scope of this work.

Nevertheless, increased electromotility from prestin overexpression appears to increase the risk of OHC loss. OHCs are known to be vulnerable to excess electromotility (Brownell 1986; Evans 1990), and the OHC plasma membrane has been identified as a target that is particularly sensitive to mechanical alteration (Chertoff and Brownell 1994; Morimoto et al. 2002; Zhi et al. 2007). We used an alternating current stimulus at acoustic frequencies to emulate the stimuli experienced by OHCs in vivo, and our findings support this concept. *Tecta*$^{C1509G/+}$ and *Tecta*$^{C1509G/C1509G}$ OHCs produced greater electromotile movements, which led to higher rates of PI labeling than their *Tecta*$^{+/+}$ counterparts.

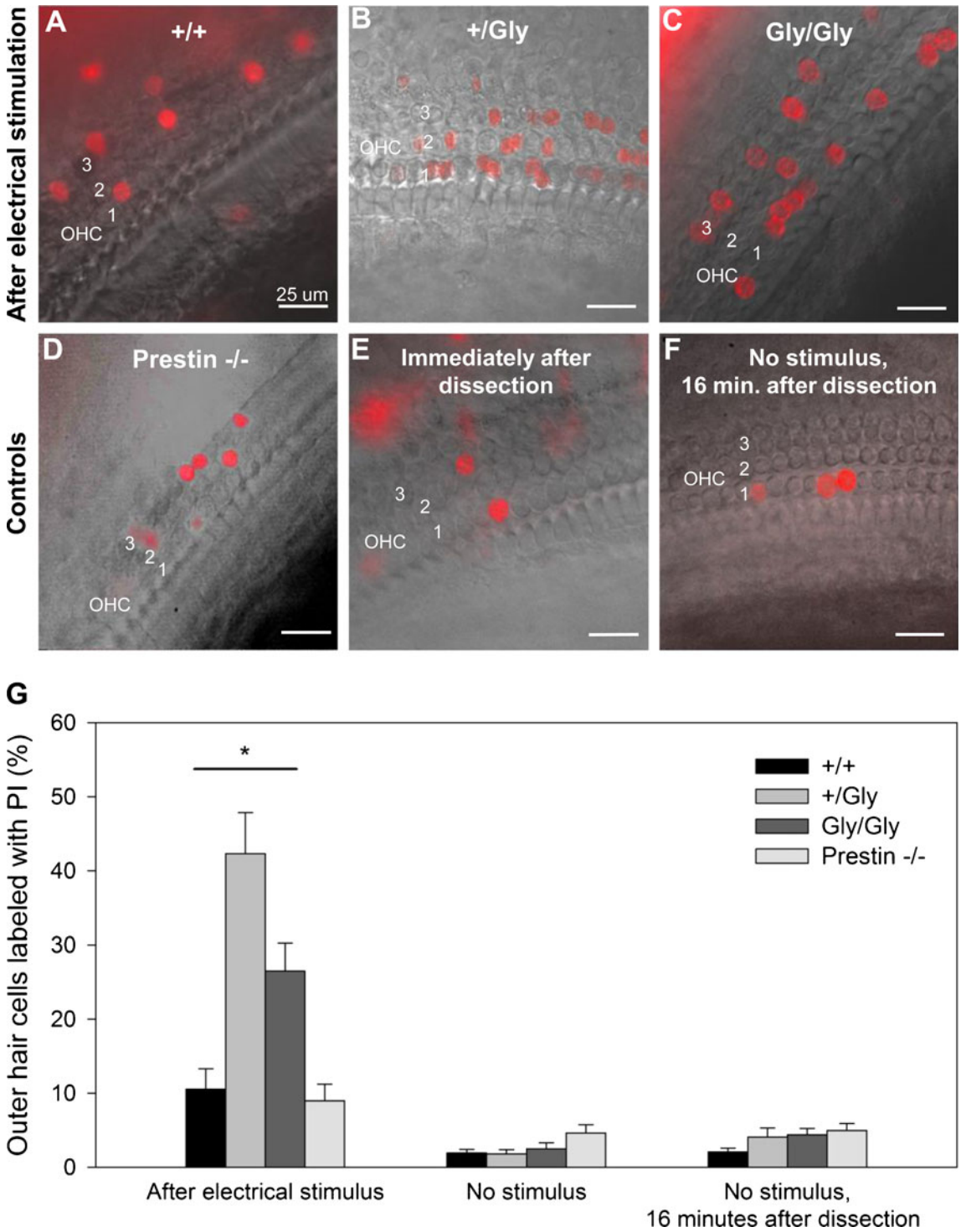


**FIG. 10.** Outer hair cell membrane compromise after electrical stimulation. **A–C** Representative images of propidium iodide-labeled OHCs immediately after electrical stimulation. The PI dye (*red*) image is superimposed over the transmitted light image of the hair cell epithelium. Note the increased labeling in *Tecta*$^{C1509G/+}$ (*+/Gly*) and *Tecta*$^{C1509G/C1509G}$ (*Gly/Gly*) OHCs compared to *Tecta*$^{+/+}$ (*+/+*) OHCs. **D** *Prestin*$^{-/-}$ cochleae were used as a control for OHC damage not related to prestin. **E** Some control cochleae were labeled with PI immediately after dissection to assess for dissection-related trauma to the OHCs. Note that very few OHCs demonstrated labeling. **F** As another control, some cochleae were immersed in artificial perilymph without stimulus application for the length of time (16 min) required to complete the stimulus cycle before application of propidium iodide. Again, it can be noted that very few OHCs demonstrated labeling. **G** The percentage of PI-labeled OHCs in *Tecta*$^{C1509G/+}$ and *Tecta*$^{C1509G/C1509G}$ cochleae was greater than the percentage of labeled OHCs in *Tecta*$^{+/+}$ and *Prestin*$^{-/-}$ cochleae (*asterisks*, ANOVA followed by non-paired Student's *t* test, $n$=11–12, $p<0.05$). Moreover, a greater proportion of *Tecta*$^{C1509G/+}$ OHCs were labeled compared to *Tecta*$^{C1509G/C1509G}$ OHCs. There was no significant increase in PI-positive cells for each genotype when cochleae were stained immediately after dissection and after 16 min in artificial perilymph (ANOVA, $n$=10–13). *Error bars* represent the SEM.

These findings agree with previous work addressing the membrane stability of prestin-expressing cells, which found that electrical stimulation of prestin was associated with membrane poration (Navarrete and Santos-Sacchi 2006).

Nanoscale movements at acoustic frequencies by prestin could affect the cell membrane and potentially increase its permeability (Chen and Zhao 2007). A corollary to this concept is that elevated prestin levels in a mutant OHC would increase this risk. This process could potentiate the large leak currents that are already present in OHCs (Beurg et al. 2009; Bian et al. 2002; Fuchs 1992; Housley and Ashmore 1992; O'Beirne and Patuzzi 2007), overwhelm a cell's ability to regulate its intracellular ion concentrations, and drive it towards necrosis or apoptosis. As well, there may be other underlying differences in the OHC membrane between *Tecta* genotypes that affect their susceptibility to electrical stimulation. For example, we do not know if there are differences in membrane components other than prestin, such as the types of phospholipids or cholesterol (Oghalai et al. 1999, 2000; Rajagopalan et al. 2007; Sfondouris et al. 2008). Further study is required to elucidate the effect of prestin on OHC membrane mechanics and stability at the molecular level.

## ACKNOWLEDGMENTS

The authors would like to thank William Brownell, Andrew Groves, Robert Raphael, Frederick Pereira, and Anping Xia for helpful comments on data interpretation. Jessica Tao and Haiying Liu provided technical assistance. Artwork was by Scott Weldon. Image processing was by Nelson Liu. This work was generously supported by the Howard Hughes Medical Institute Medical Fellows Program, NIH grants DC006671, DC07910, P30 DC010363, and DOD CDMRP grant DM090212.

## REFERENCES

ALASTI F, SANATI MH, BEHROUZIFARD AH, SADEGHI A, DE BROUWER AP, KREMER H, SMITH RJ, VAN CAMP G (2008) A novel TECTA mutation confirms the recognizable phenotype among autosomal recessive hearing impairment families. Int J Pediatr Otorhinolaryngol 72:249–255

BEURG M, FETTIPLACE R, NAM J, RICCI A (2009) Localization of inner hair cell mechanotransducer channels using high-speed calcium imaging. Nat Neurosci 12:553–558

BIAN J, YEH J, AISTRUP G, NARAHASHI T, MOORE E (2002) Inhibition of K+currents of outer hair cells in guinea pig cochlea by fluoxetine. Eur J Pharmacol 453:159–166

BROWNELL WE (1986) Outer hair cell motility and cochlear frequency selectivity. In: Moore BCJ, Patterson RD (eds) Auditory frequency selectivity. Plenum Press, New York

BROWNELL W (1990) Outer hair cell electromotility and otoacoustic emissions. Ear Hear 11:82–92

BROWNELL W, BADER C, BERTRAND D, DE RIBAUPIERRE Y (1985) Evoked mechanical responses of isolated cochlear outer hair cells. Science 227:194–196

CANLON B (1987) Acoustic overstimulation alters the morphology of the tectorial membrane. Hear Res 30:127–134

CANLON B (1988) The effect of acoustic trauma on the tectorial membrane, stereocilia, and hearing sensitiviy: possible mechanisms underlying damage, recovery, and protection. Scand Audiol Suppl 27:1–45

CHAN D, HUDSPETH A (2005A) Mechanical responses of the organ of Corti to acoustic and electrical stimulation in vitro. Biophys J 89:4382–4395

CHAN D, HUDSPETH A (2005B) Ca2+ current-driven nonlinear amplification by the mamalian cochlea in vitro. Nat Neurosci 8:149–155

CHEN G, FECHTER L (2003) The relationship between noise-induced hearing loss and hair cell loss in rats. Hear Res 177:81–90

CHEN G, ZHAO H (2007) Effects of intense noise exposure on the outer hair cell plasma membrane fluidity. Hear Res 226:14–21

CHEN Y, LIU T, CHENG C, YEH T, LEE S, HSU C (2003) Changes of hair cell stereocilia and threshold shift after acoustic trauma in guinea pigs: comparison between inner and outer hair cells. ORL J Otorhinolaryngol Relat Spec 65:266–274

CHERTOFF ME, BROWNELL WE (1994) Characterization of cochlear outer hair cell turgor. Am J Physiol 266:C467–C479

CHOI CH, OGHALAI JS (2008) Perilymph osmolality modulates cochlear function. The Laryngoscope 118:1621–1629

CLARK J, PICKLES J (1996) THe effects of moderate and low levels of acoustic overstimulation on stereocilia and their tip links in the guinea pig. Hear Res 99:119–128

COLLIN RW, DE HEER AM, OOSTRIK J, PAUW RJ, PLANTINGA RF, HUYGEN PL, ADMIRAAL R, DE BROUWER AP, STROM TM, CREMERS CW, KREMER H (2008) Mid-frequency DFNA8/12 hearing loss caused by a synonymous TECTA mutation that affects an exonic splice enhancer. Eur J Hum Genet 16:1430–1436

CRISTOBAL B, OGHALAI J (2008) Hearing loss in children with very low birth weight: current review of epidemiology and pathophysiology. Arch Dis Child Fetal Neonatal Ed 93:462–468

DALLOS P (2008) Cochlear amplification, outer hair cells and prestin. Curr Opin Neurobiol 18:370–376

DALLOS P, ZHENG J, CHEATHAM MA (2006) Prestin and the cochlear amplifier. J Physiol 576:37–42

DAVIS H (1983) An active process in cochlear mechanics. Hear Res 9:79–90

DAVIS R, KOZEL P, ERWAY L (2003) Genetic influences in individual susceptibility to noise: a review. Noise Health 5:19–28

DEO N, GROSH K (2004) Two-state model for outer hair cell stiffness and motility. Biophys J 86:3519–3528

EVANS BN (1990) Fatal contractions: ultrastructural and electromechanical changes in outer hair cells following transmembraneous electrical stimulation. Hear Res 45:265–282

FETTIPLACE R (2009) Defining features of the hair cell mechanoelectrical transducer channel. Pflugers Arch 458:1115–1123

FROLENKOV G, BELYANTSEVA I, KURC M, MASTROIANNI M, KACHAR B (1998) Cochlear outer hair cell electromotility can provide force for both low and high intensity distortion product otoacoustic emissions. Hear Res 126:67–74

FUCHS P (1992) Ionic currents in cochlear hair cells. Prog Neurobiol 39:439–505

GATES G, SCHMID P, KUJAWA S, NAM B, D'AGOSTINO R (2000) Longitudinal threshold changes in older men with audiometric notches. Hear Res 141:220–228

GAVARA N, CHADWICK RS (2009) Collagen-based mechanical anisotropy of the tectorial membrane: implications for inter-row coupling of outer hair cell bundles. PLoS ONE 4:e4877

GHAFFARI R, ARANYOSI A, FREEMAN D (2007) Longitudinally propagating traveling waves of the mammalian tectorial membrane. Proc Natl Acad 104:16510–16515

GOODYEAR R, RICHARDSON G (2002) Extracellular matrices associated with the apical surfaces of sensory epithelia in the inner ear: molecular and structural diversity. J Neurobiol 53:212–227

Govaerts PJ, De Ceulaer G, Daemers K, Verhoeven K, Van Camp G, Schatteman I, Verstreken M, Willems PJ, Somers T, Offeciers FE (1998) A new autosomal-dominant locus (DFNA12) is responsible for a nonsyndromic, midfrequency, prelingual and nonprogressive sensorineural hearing loss. Am J Otol 19:718–723

Gu JW, Hemmert W, Freeman DM, Aranyosi AJ (2008) Frequency-dependent shear impedance of the tectorial membrane. Biophys J 95:2529–2538

Gueta R, Barlam D, Shneck RZ, Rousso I (2006) Measurement of the mechanical properties of isolated tectorial membrane using atomic force microscopy. Proc Natl Acad Sci USA 103:14790–14795

Gueta R, Tal E, Silberberg Y, Rousso I (2007) The 3D structure of the tectorial membrane determined by second-harmonic imaging microscopy. J Struct Biol 159:103–110

Gueta R, Barlam D, Shneck RZ, Rousso I (2008) Sound-evoked deflections of outer hair cell stereocilia arise from tectorial membrane anisotropy. Biophys J 94:4570–4576

Hackney C, Mahendrasingam S, Penn A, Fettiplace R (2005) The concentrations of calcium buffering proteins in mammalian cochlear hair cells. J Neurosci 25:7867–7875

He D, Jia S, Dallos P (2003) Prestin and the dynamic stiffness of cochlear outer hair cells. J Neuroscience 23(27):9089–9096

Holme R, Steel K (2004) Progressive hearing loss and increased susceptibility to noise-induced hearing loss in mice carrying a Cdh23 but not a Myo7a mutation. J Assoc Res Otolaryngol 5:66–79

Housley G, Ashmore J (1992) Ionic currents of outer hair cells isolated from the guinea-pig cochlea. J Physiol 448:73–98

Hudspeth AJ (2008) Making an effort to listen: mechanical amplification in the ear. Neuron 59:530–545

Iwasaki S, Harada D, Usami S, Nagura M, Takeshita T, Hoshino T (2002) Association of clinical features with mutation of TECTA in a family with autosomal dominant hearing loss. Arch Otolaryngol Head Neck Surg 128:913–917

Karchmer M, Allen T (1999) The functional assessment of deaf and hard of hearing students. Am Ann Deaf 144:68–77

Kennedy H, Evans M, Crawford A, Fettiplace R (2006) Depolarization of cochlear outer hair cells evokes active hair bundle motion by two mechanisms. J Neurosci 26:2757–2766

Kiang NY, Liberman MC, Sewell WF, Guinan JJ (1986) Single unit clues to cochlear mechanisms. Hear Res 22:171–182

Kirschhofer K, Kenyon JB, Hoover DM, Franz P, Weipoltshammer K, Wachtler F, Kimberling WJ (1998) Autosomal-dominant, prelingual, nonprogressive sensorineural hearing loss: localization of the gene (DFNA8) to chromosome 11q by linkage in an Austrian family. Cytogenet Cell Genet 82:126–130

Kujawa S, Liberman M (2006) Acceleration of age-related hearing loss by early noise exposure: evidence of a misspent youth. J Neurosci 26:2115–2123

Kurian R, Krupp N, Saunders J (2003) Tip link loss and recovery on chick short hair cells following intense exposure to sound. Hear Res 181(1–2):40–50

Kushalnagar P, Krull K, Hannay J, Mehta P, Caudle S, Oghalai J (2007) Intelligence, parental depression, and behavior adaptability in deaf children being considered for cochlear implantation. J Deaf Stud Deaf Educ 12:335–349

Leibovici M, Safieddine S, Petit C (2008) Mouse models for human hereditary deafness. Curr Top Dev Biol 84:385–429

Liberman M, Gao J, He D, Wu X, Jia S, Zuo J (2002) Prestin is required for electromotility of the outer hair cell and for the cochlear amplifier. Nature 419:300–304

Lim D (1986) Effects of noise and ototoxic drugs at the cellular level in the cochlea: a review. Am J Otolaryngol 7:73–99

Lim H, Choi S, Kang H, Ahn J, Chung J (2008) Apoptotic pattern of cochlear outer hair cells and frequency-specific hearing threshold shift in noise-exposed BALB/c mice. Clin Exp Otorhinolaryngol 1:80–85

Liu Y, Neely S (2009) Outer hair cell electromechanical properties in a nonlinear piezoelectric model. J Acoust Soc Am 126:751–761

Lue A, Brownell W (1999) Salicylate induced changes in outer hair cell lateral wall stiffness. Hear Res 135:163–168

Masaki K, Gu J, Ghaffari R, Chan G, Smith R, Freeman D, Aranyosi A (2009) Col11a2 deletion reveals the molecular basis for tectorial membrane mechanical anisotropy. Biophys J 96:4717–24

Masaki K, Ghaffari R, Gu JW, Richardson GP, Freeman DM, Aranyosi AJ (2010) Tectorial membrane material properties in Tecta(Y) (1870C/+) heterozygous mice. Biophys J 99:3274–3281

Meaud J, Grosh K (2010) The effect of tectorial membrane and basilar membrane longitudinal coupling in cochlear mechanics. J Acoust Soc Am. 127(3):1411–21

Minami S, Yamashita D, Schacht J, Miller J (2004) Calcineurin activation contributes to noise-induced hearing loss. J Neurosci Res 78:383–392

Moreno-Pelayo MA, del Castillo I, Villamar M, Romero L, Hernandez-Calvin FJ, Herraiz C, Barbera R, Navas C, Moreno F (2001) A cysteine substitution in the zona pellucida domain of alpha-tectorin results in autosomal dominant, postlingual, progressive, mid frequency hearing loss in a Spanish family. J Med Genet 38:E13

Morimoto N, Raphael RM, Nygren A, Brownell WE (2002) Excess plasma membrane and effects of ionic amphipaths on mechanics of outer hair cell lateral wall. Am J Physiol 282:C1076–C1086

Muller M, von Hunerbein K, Hoidis S, Smolders J (2005) A physiological place-frequency map of the cochlea in the CBA/J mouse. Hear Res 202:63–73

Navarrete E, Santos-Sacchi J (2006) On the effect of prestin on the electrical breakdown of cell membranes. Biophys J 90:967–974

Nordmann A, Bohne B, Harding G (2000) Histopathological differences between temporary and permanent threshold shift. Hear Res 139:13–30

O'Beirne G, Patuzzi R (2007) Mathematical model of outer hair cell regulation including ion transport and cell motility. Hear Res 234:29–51

Oghalai JS (2004a) The cochlear amplifier: augmentation of the traveling wave within the inner ear. Curr Opin Otolaryngol Head Neck Surg 12:431–438

Oghalai JS (2004b) Chlorpromazine inhibits cochlear function in guinea pigs. Hear Res 198:59–68

Oghalai JS, Patel AA, Nakagawa T, Brownell WE (1998) Fluorescence-imaged microdeformation of the outer hair cell lateral wall. J Neurosci 18:48–58

Oghalai JS, Tran TD, Raphael RM, Nakagawa T, Brownell WE (1999) Transverse and lateral mobility in outer hair cell lateral wall membranes. Hear Res 135:19–28

Oghalai JS, Zhao HB, Kutz JW, Brownell WE (2000) Voltage- and tension-dependent lipid mobility in the outer hair cell plasma membrane. Science 287:658–661

Ohlemiller K (2008) Recent findings and emerging questions in cochlear noise injury. Hear Res 245:5–17

Peleg U, Perez R, Freeman S, Sohmer H (2007) Salicylate ototoxicity and its implications for cochlear microphonic potential generation. J Basic Clin Physiol Pharmacol 18:173–188

Petit C, Richardson GP (2009) Linking genes underlying deafness to hair-bundle development and function. Nat Neurosci 12:703–710

Pfister MHT, Van Camp G, Fransen E, Apaydin F, Aydin O, Leistenschneider P, Devoto M, Zenner H, Blin N, Nurnberg P, Ozkarakas H, Kupka S (2004) A genotype–phenotype correlation with gender-effect for hearing impairment caused by TECTA mutations. Cell Physiol Biochem 14:369–376

Pierson S, Caudle S, Krull K, Haymond J, Tonini RJS (2007) Cognition in children with sensorineural hearing loss: etiologic considerations. Laryngoscope 117:1661–1665

PLANTINGA RF, DE BROUWER AP, HUYGEN PL, KUNST HP, KREMER H, CREMERS CW (2006) A novel TECTA mutation in a Dutch DFNA8/12 family confirms genotype–phenotype correlation. J Assoc Res Otolaryngol 7(2):173–81

POLOGRUTO T, SABATINI B, SVOBODA K (2003) ScanImage: flexible software for operating laser scanning microscopes. Biomed Eng Online 17:2–13

QIU Y, PEREIRA F, DEMAYO F, LYDON J, TSAI S, TSAI M (1997) Null mutation of mCOUP-TFI results in defects in morphogenesis of the glossopharyngeal ganglion, axonal projection, and arborization. Genes Dev 11:1925–1937

RAJAGOPALAN L, GREESON J, XIA A, LIU H, STURM A, RAPHAEL R, DAVIDSON A, OGHALAI J, PEREIRA F, BROWNELL W (2007) Tuning of the outer hair cell motor by membrane cholesterol. J Biol Chem 282:36659–36670

RAU A, LEGAN P, RICHARDSON G (1999) Tectorin mRNA expression is spatially and temporally restricted during mouse inner ear development. J Comp Neurol 405:271–280

REUTER G, GITTER A, THURM U, ZENNER H (1992) High frequency radial movements of the reticular lamina induced by outer hair cell motility. Hear Res 60:236–246

RICHTER C, EMADI G, GETNICK G, QUESNEL A, DALLOS P (2007) Tectorial membrane stiffness gradients. Biophys J 93:2265–2276

ROSENHALL U (2003) The influence of aging on noise-induced hearing loss. Noise Health 5:47–53

SAKAGUCHI H, TOKITA J, MULLER U, KACHAR B (2009) Tip links in hair cells: molecular composition and role in hearing loss. Curr Opin Otolaryngol Head Neck Surg 17:388–393

SEIDMAN M, AHMAD N, BAI U (2002) Molecular mechanisms of age-related hearing loss. Ageing Res Rev 1:331–343

SFONDOURIS J, RAJAGOPALAN L, PEREIRA F, BROWNELL W (2008) Membrane composition modulates prestin-associated charge movement. J Biol Chem 283:22473–22481

SHOELSON B, DIMITRIADIS EK, CAI H, KACHAR B, CHADWICK RS (2004) Evidence and implications of inhomogeneity in tectorial membrane elasticity. Biophys J 87:2768–2777

STASIUNAS A, VERIKAS A, MILIAUSKAS R, STASIUNIENE N (2009) An adaptive model simulating the somatic motility and the active hair bundle motion of the OHC. Comput Biol Med 39:800–809

STEELE CR, PURIA S (2005) Force on inner hair cell cilia. Int J Solids Struct 42:5887–5904

STEELE CR, BOUTET DE MONVEL J, PURIA S (2009) A multiscale model of the organ of Corti. J Mech Mater Struct 4:755–778

STEELE C, O'CONNOR KN, PURIA S (2010) Modeling the effects of organ of Corti cytoarchitectural modifications, Association for Research in Otolaryngology abstract # 1037

SZONYI M, HE D, RIBARI O, SZIKLAI I, DALLOS P (2001) Intracellular calcium and outer hair cell electromotility. Brain Res 922:65–70

TOMO I, BOUTET DE MONVEL J, FRIDBERGER A (2007) Sound-evoked radial strain in the hearing organ. Biophys J 93:3279–3284

VERHOEVEN K, VAN LAER L, KIRSCHHOFER K, LEGAN PK, HUGHES DC, SCHATTEMAN I, VERSTREKEN M, VAN HAUWE P, COUCKE P, CHEN A, SMITH RJ, SOMERS T, OFFECIERS FE, VAN DE HEYNING P, RICHARDSON GP, WACHTLER F, KIMBERLING WJ, WILLEMS PJ, GOVAERTS PJ, VAN CAMP G (1998) Mutations in the human alpha-tectorin gene cause autosomal dominant non-syndromic hearing impairment. Nat Genet 19:60–62

VIBERG A, CANLON B (2004) The guide to plotting a cochleogram. Hear Res 197:1–10

VICENTE-TORRES M, SCHACHT J (2006) A BAD link to mitochondrial cell death in the cochlea of mice with noise-induced hearing loss. J Neurosci Res 83:1564–1572

XIA A, VISOSKY A, CHO J, TSAI M, PEREIRA F, OGHALAI J (2007) Altered traveling wave propagation and reduced endocochlear potential associated with cochlear dysplasia in the BETA2/NeuroD1 null mouse. J Assoc Res Otolaryngol 8:447–463

XIA A, GAO S, YUAN T, OSBORN A, BRESS A, PFISTER M, MARICICH S, PEREIRA F, OGHALAI J (2010) Deficient forward transduction and enhanced reverse transduction in the alpha tectorin C1509G human hearing loss mutation. Dis Model Mech 3:209–223

YOON YJ, PURIA S, STEELE CR (2006) Intracochlear pressure and organ of Corti impedance from a linear active three-dimensional model. ORL 68:365–372

YOON YJ, PURIA S, STEELE CR (2007) Intracochlear pressure and derived quantities from a three-dimensional model. J Acoust Soc Am 122:952–966

YOON Y, PURIA S, STEELE CR (2009) A cochlear model using the time-averaged lagrangian and the push–pull mechanism in the organ of Corti. J Mech Mater Struct 4:977–986

YOSHIDA N, HEQUEMBOURG S, ATENCIO CA, ROSOWSKI JJ, LIBERMAN MC (2000) Acoustic injury in mice: 129/SvEv is exceptionally resistant to noise-induced hearing loss. Hear Res 141:97–106

YU N, ZHAO H (2009) Modulation of outer hair cell electromotility by cochlear supporting cells and gap junctions. PLoS ONE 4: e7923

YU N, ZHU M, JOHNSON B, LIU Y, JONES R, ZHAO H (2008) Prestin-upregulation in chronic salicylate (aspirin) administration: an implication of functional dependence of prestin expression. Cell Physiol Biochem 65:2407–2418

YUAN T, GAO S, SAGGAU P, OGHALAI J (2010) Calcium imaging of inner ear hair cells within the cochlear epithelium of mice using two-photon microscopy. J Biomed Opt 15:016002

ZHAO H, SANTOS-SACCHI J (1999) Auditory collusion and a coupled couple of outer hair cells. Nature 399:359–362

ZHENG J, SHEN W, HE DZ, LONG KB, MADISON LD, DALLOS P (2000) Prestin is the motor protein of cochlear outer hair cells. Nature 405:149–155

ZHI M, RATNANATHER JT, CEYHAN E, POPEL AS, BROWNELL WE (2007) Hypotonic swelling of salicylate-treated cochlear outer hair cells. Hear Res 228:95–104